Journal of Biomedical Optics

BiomedicalOptics.SPIEDigitalLibrary.org

Modulation of ultrasound-switchable fluorescence for improving signal-to-noise ratio

Jayanth Kandukuri
Shuai Yu
Tingfeng Yao
Baohong Yuan

SPIE.

Jayanth Kandukuri, Shuai Yu, Tingfeng Yao, Baohong Yuan, "Modulation of ultrasound-switchable fluorescence for improving signal-to-noise ratio," *J. Biomed. Opt.* **22**(7), 076021 (2017), doi: 10.1117/1.JBO.22.7.076021.

Journal of Biomedical Optics 22(7), 076021 (July 2017)

Modulation of ultrasound-switchable fluorescence for improving signal-to-noise ratio

Jayanth Kandukuri,[a,b] Shuai Yu,[a,b] Tingfeng Yao,[a,b] and Baohong Yuan[a,b,*]
[a]University of Texas at Arlington, Ultrasound and Optical Imaging Laboratory, Department of Bioengineering, Arlington, Texas, United States
[b]University of Texas at Arlington and University of Texas Southwestern Medical Center at Dallas, Joint Biomedical Engineering Program, Dallas, Texas, United States

Abstract. Simultaneously achieving high signal-to-noise ratio (SNR) (or sensitivity) and high resolution is desired in biomedical imaging. However, conventional imaging modality has a tradeoff between SNR (or sensitivity) and resolution. We developed a method to simultaneously achieve high SNR (or sensitivity) and high resolution for fluorescence imaging in deep tissue. We first introduce a recently developed deep-tissue high-resolution imaging technique termed as ultrasound-switchable fluorescence (USF). An approach of modulating ultrasound exposure time is adopted to increase the detectability of the USF signal. The control parameters of modulation of ultrasound—such as (1) frequency, (2) duty cycle, and (3) exposure duration—are varied to study their influence on the USF signal and SNR. We conclude that high SNR can be achieved by modulating ultrasound exposure without sacrificing the spatial resolution. This is important for future fluorescence molecular imaging of cancer in deep tissue. [DOI: 10.1117/1.JBO.22.7.076021]

Keywords: ultrasound-switchable fluorescence; modulation; biomedical imaging; deep-tissue fluorescence imaging.

Paper 170298R received May 8, 2017; accepted for publication Jul. 14, 2017; published online Jul. 31, 2017.

1 Introduction

Achieving both high signal-to-noise ratio (SNR) (or sensitivity) and high spatial resolution in deep tissue is highly desired in biomedical imaging.[1–4] However, conventional imaging modality has a tradeoff between SNR (or sensitivity) and resolution.[1–6] We recently developed a new imaging method for deep-tissue high-resolution imaging, which has been termed as ultrasound-switchable fluorescence (USF).[7–13] It has been demonstrated that USF can simultaneously achieve high SNR (or sensitivity) and high spatial resolution in tissue with a depth of centimeters.[7–13] In this study, we report a new method to further improve the SNR (or sensitivity) of the USF imaging without sacrificing the spatial resolution by modulating the ultrasound exposure. The modulation parameters and data processing methods are also investigated and compared.

The principle of USF imaging has been described in our recent publications.[7–13] For integrity, it is briefly introduced here. Two major components are included in USF imaging: (1) USF contrast agents and (2) an imaging system. When environment-sensitive fluorophores are conjugated on a thermosensitive polymer or encapsulated into a thermosensitive nanoparticle, the fluorescence intensity exhibits a switch-like function of the temperature. Below a temperature threshold (T_{th1}), the fluorophores either do not fluoresce or very weakly (i.e., at off state). When the temperature is above another threshold (T_{th2}), the fluorophores are completely switched on and emit strongly (i.e., at on state). Generally, the temperature difference between T_{th2} and T_{th1} is small (such as a few Celsius degrees). By using a highly focused ultrasound transducer to illuminate tissue, the temperature in the focal volume can be quickly increased a few Celsius degrees compared with the temperature outside the focal volume due to the tissue absorption of the ultrasound energy. Accordingly, the USF contrast agents within the focal volume can be switched on and generate fluorescence photons, which is called USF photons. Meanwhile, the contrast agents outside the focal volume remain off because the temperature is lower than the threshold (T_{th1}). By scanning the ultrasound focus point-by-point in the tissue, a high-resolution USF image can be generated. It has been well known that diffused (i.e., highly scattered) near-infrared light can penetrate tissue several centimeters.[14] Therefore, USF imaging can achieve the similar depth.[7–13]

We hypothesize that the SNR (or sensitivity) of the USF imaging can be improved by modulating ultrasound exposure via gating the high-intensity focused ultrasound (HIFU) transducer. The gating signal applied on the transducer switches on and off the ultrasound exposure at a certain frequency, which further leads to the modulation of the temperature and the USF signal within the focal volume of the transducer. By detecting the modulated USF signal at this specific modulation frequency, the SNR (or sensitivity) can be increased.

2 Ultrasound-Switchable Fluorescence Imaging System

2.1 *Hardware of the System*

The diagram of the USF imaging system is shown in Fig. 1(a). The major components have been introduced in our previous publication.[11,12] For integrity, we will very briefly introduce the entire system and emphasize the difference between the current system and the previous ones.[11,12] Similar to the previous ones,[11,12] the current USF subsystem includes the following modules: (1) an ultrasound heating and its driving module,

*Address all correspondence to: Baohong Yuan, E-mail: baohong@uta.edu

1083-3668/2017/$25.00 © 2017 SPIE

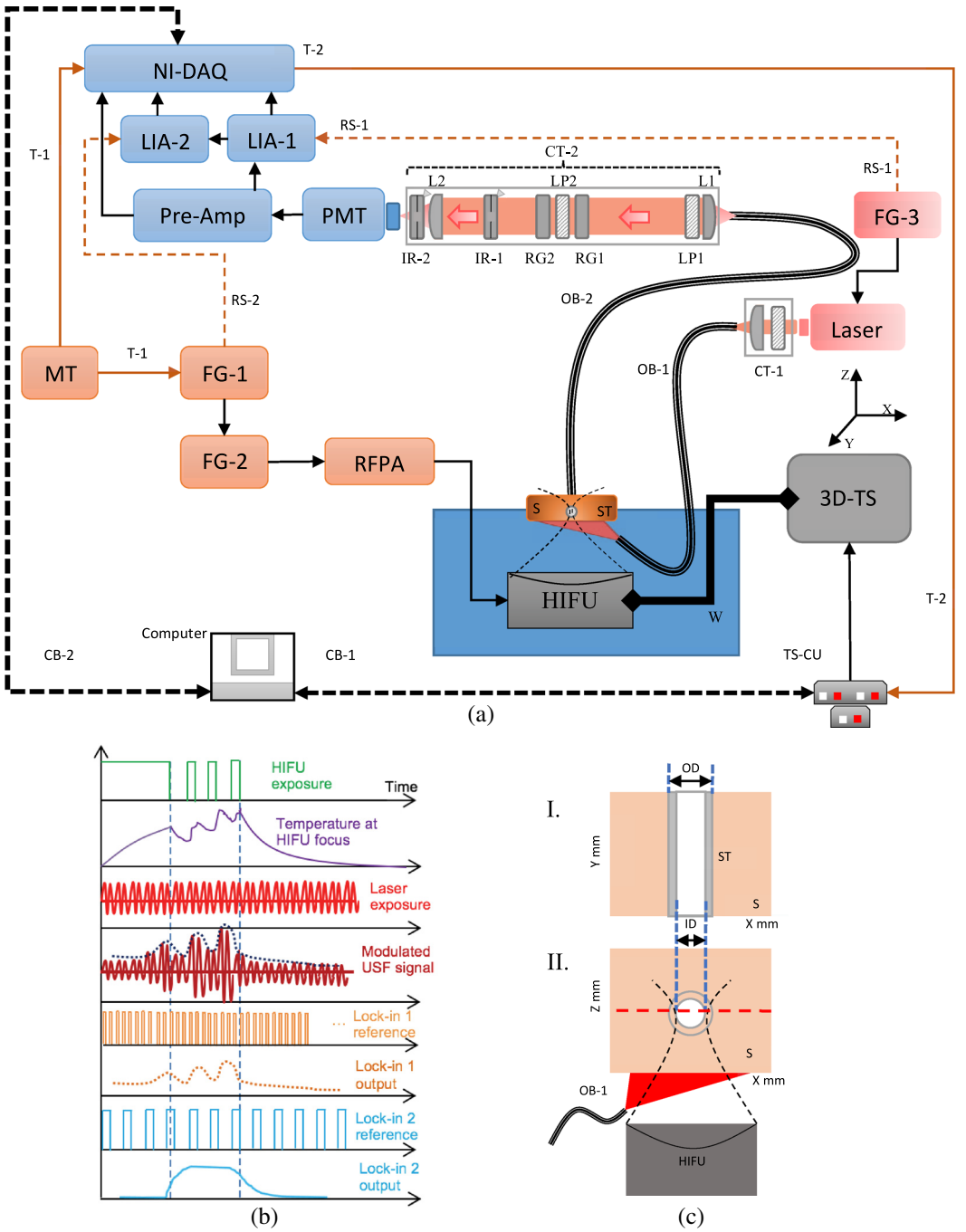

Fig. 1 (a) The experiment block diagram. (b) A schematic diagram of the time sequence of different signals. (c) Sample configuration including *x*–y (horizontal) and *x*–z (vertical) regions of USF Imaging. MT: a pulse delay generator serves as an MT (T-1) with 0.1-Hz frequency; FG-1: a function generator for gating the second function generator FG-2 to drive the HIFU transducer module (2.5 MHz; HIFU), and generating a reference signal (RS-2) to LIA-2; FG-2: a function generator for driving the HIFU transducer by generating a 2.5 MHz sinusoidal signal and amplified by an RFPA; FG-3: a function generator to modulate the excitation laser at a 1-kHz frequency and generate a reference signal (RS-1) for the lock-in amplifier; W: a water tank to immerse the HIFU transducer and partially immerse the sample (S); ST: a silicone tube with an inner diameter (ID) of 0.31 mm and an outer diameter (OD) of 0.64 mm; 3D-TS: the three-dimensional (3-D) translational stages; TS-CU: 3-D translational stage motorized control units; CT-1: a collimation tube to focus the excitation laser into an optical bundle (OB-1); CT-2: an optimized collimation tube to guide the collected fluorescence from the optical bundle (OB-2) to the photodetector (PMT) and best eliminate the excitation light and pass the emission light; PMT: a photomultiplier tube to detect the optical fluorescence signal; Preamp: a preamplifier to amplify and filter the signal from the PMT; Laser: a 671-nm laser to irradiate the sample (S); LIA-1: a lock-in amplifier to detect the 1-kHz optical signal; LIA-2: a second lock-in amplifier to detect the signal with the HIFU-modulation frequency; NI-DAQ: a national instrument data acquisition card; CB-1: serial communication bus to control TS-MCU; CB-2: communication bus to transfer data; RS-1: a 1-KHz reference signal for LIA-1; RS-2: a reference signal with the modulation frequency for LIA-2; T-1: a trigger signal for the NIDAQ card; T-2: a single cycle digital pulse signal to trigger the movement of the 3D-TS.

(2) an excitation light source, (3) a sample module, (4) an optical detection module, and (5) a scanning module.

2.1.1 *Ultrasound heating and its driving module*

A single-element and water immersible HIFU transducer (H-108) was purchased from Sonic Concepts Ltd (Bothell, Washington), as shown in Fig. 1(a). It has a geometric focal length of ~50 mm and a central frequency of 2.5 MHz. Based on the manufacturer provided data, the lateral and axial pressure focal size are 0.51 and 3.28 mm, respectively. The HIFU transducer is driven by a function generator (FG-2, Agilent 33500B, Chicago, Illinois) and a radio-frequency power amplifier (RFPA; 325LA, Electronics & Innovation, New York). The exposure power of the HIFU transducer can be controlled by varying the peak-to-peak voltage (V_{pp}) of the 2.5-MHz sinusoidal wave from the FG-2. The exposure duration of the HIFU transducer is controlled by the width of the gating pulse train from another function generator (FG-1, AFG 3252, Tektronix, Texas). The FG-1 has two channels. The first channel of the FG-1 generates a gating pulse train that switches the FG-2 on and off. The number of pulses, the pulse width, and the frequency ($f_{\text{M-HIFU}}$) can be programmed into the FG-1 and varied to generate different modulation patterns. The FG-1 is triggered by a pulse-delay generator (DG645, Stanford Research, Sunnyvale, California), which acts as a master trigger (MT) for the entire system, as shown in Fig. 1. MT is also responsible for triggering the data acquisition module to record data and will be discussed shortly. The second channel of the FG-1 is programmed to generate a continuous pulse train with the same frequency as the first channel ($f_{\text{M-HIFU}}$). This continuous pulse train is used as the reference for a lock-in amplifier (LIA-2; SR830, Stanford Research) to detect the HIFU-modulated USF signal. Note that the locked frequency by LIA-2 is $f_{\text{M-HIFU}}$ and is called HIFU-modulation frequency (because it is the modulation frequency of the HIFU exposure), which is different from the optical modulation frequency discussed in next paragraph.

2.1.2 *Excitation light source*

Similar to the previous systems,[11,12] a 671-nm laser (MLL-FN-671-500 mW, Optoengine LLC, Midvale, Utah) was used as the excitation light and delivered to the bottom of the sample via a fiber bundle (optical bubdle, OB-1). A bandpass filter of 671/11 nm (FF01-673/11-25, Semrock, Rochester, New York) was placed in front of the laser head to remove any unknown laser lines from the laser. The laser intensity was modulated into a sinusoidal wave at 1 kHz via the third function generator (FG-3, 33220A, Agilent). The synchronized output (a 1-kHz square wave) from another channel of the FG-3 was used as a reference signal for another LIA-1 (SR830, Stanford Research) for detecting the 1-kHz fluorescence signal. Note that the locked frequency by LIA-1 is 1 kHz and is called optical modulation frequency ($f_{\text{M-OPT}}$) (because it is the modulation frequency of the optical exposure), which should not be confounded with the previously discussed HIFU-modulation frequency ($f_{\text{M-HIFU}}$).

2.1.3 *Sample configuration*

A silicone tube (ST; 60-011-01, Hellix Medical, Carpinteria, California) was filled with the solution of a USF contrast agent and embedded into a piece of porcine muscle tissue [Figs. 1(a) and 1(c)]. Part I in Fig. 1(c) shows the $x-y$ (horizontal) plane, which is the region scanned by the HIFU transducer using the three motorized linear translational stages (3D-TS) system (the USF images obtained in Figs. 5 and 7 correspond to this scanning area). Part II in Fig. 1(c) shows the x–z (vertical) plane that indicates how the same sample and the embedded tube are arranged with respect to the HIFU transducer and the illumination of laser via OB-1. The thickness of the muscle tissue was ~12 mm. The tube with an inner diameter (ID) of 0.31 mm and an outer diameter (OD) of 0.64 mm was located around the middle along the depth direction. The USF contrast agent is pluronic F98 nanocapsules in which fluorophores of aza-BODIPY conjugated with two hydroxyls at the bottom [denoted as ADP(OH)_2] were encapsulated.[11,12]

2.1.4 *Optical detection module*

Similar to the previous systems,[11,12] the emission photons were collected via another fiber bundle (OB-2) positioned on the top of the tissue sample. The collected photons were delivered to a collimation and filtering system for collimating the scattered photons and blocking the excitation light. This system consisted of the following components: (1) two NIR planoconvex lenses for collimation (L1 and L2, AC254-030-B, Thorlabs, Newton, New Jersey), (2) two interference and two absorption filters for blocking exciting light (LP1 and LP2: 715-nm long-pass interference filters, FF01-715/LP-25, Semrock, Rochester, New York; RG1 and RG2: 695 nm long-wave pass cut-on filters, FSR-RG695, Newport, Irvine, CA, USA), and (3) two irises (IR1 and IR2, SM1D12SZ, Thorlabs) for protecting the photodetector by closing the optical path when needed and also controlling the aperture size for further blocking the background photons. The photons were eventually converted into electronic signal by a cooled photomultiplier tube (PMT, H7422-20, Hamamatsu, Bridgewater, New Jersey) and further amplified by a low-noise preamplifier (Pre-Amp; SR570, Stanford Research). The electronic signal was input into the first LIA-1 (SR830, Stanford Research) for detecting the amplitude variation of the 1-kHz signal using the synchronized reference signal from the FG-3 (RS-1, at the same frequency of $f_{\text{M-OPT}} = 1$ kHz).

In general, the 1-kHz optical signal consisted of both USF signal and background noise. As discussed previously,[11,12] the background noise mainly originated from: (1) laser leakage, (2) autofluorescence from the sample, and/or (3) fluorescence from those non-100%-off USF contrast agents. Fortunately, all these three components of the noise were independent of ultrasound. By contrast, the USF signal was uniquely controlled by the ultrasound (i.e., HIFU-induced temperature). Accordingly, the dynamic variation of the amplitude of the 1-kHz signal should follow the similar pattern as the variation of the HIFU-induced temperature. When the HIFU exposure was modulated with a central frequency of $f_{\text{M-HIFU}}$, the variation of the USF signal should have the same frequency. To sensitively detect this USF signal with the frequency of $f_{\text{M-HIFU}}$, the output of the first LIA-1 was given as input to the second LIA-2 (SR830, Stanford Research). Reference for the LIA-2 (denoted as RS-2) was given from channel 2 of the FG-1 with the frequency of $f_{\text{M-HIFU}}$. Note that, in this study, the value of $f_{\text{M-HIFU}}$ was investigated based on SNR. The time constant of LIA was set to <300 ms and the sensitivity varied from 50 to 500 mV nA depending upon the modulation pattern and

signal strength. A national instrument data acquisition card (NI-DAQ; PCIE-6363, National Instruments, Dallas, Texas) was used to acquire the signals from both LIA-1 and LIA-2. The relationship among the modulation of the HIFU exposure, the HIFU-induced temperature modulation, the modulated excitation light, the modulated USF signal, the lock-in references, and the outputs of the LIA-1 and LIA2 is schematically displayed in Fig. 1(b).

2.1.5 *Scanning module*

The scanning module was the same as previous systems.[11,12] Briefly, 3D-TS were orthogonally stacked together to have a three-dimensional (3-D) scanning capability [although in this study we only used two-dimensional (2-D) scanning] and controlled by the three-axis programmable stepping motor controller (TS-CU). The controller was connected to a computer. A MATLAB GUI was programed to control the controller and further scan the HIFU transducer for acquiring USF images (in this study, only 2-D image was scanned).

2.2 *System Operational Flow Diagram*

The system operational flow diagram is shown in Fig. 2. An MT started the entire system by triggering both the FG1 and the NI-DAQ. The typical duration of the optical signal acquisition was 4 to 8 s. Once all the data were acquired and stored, the MATLAB GUI will generate a voltage pulse via the output port of the NI-DAQ and trigger the Velmex 3-D translational stages to move to the next location. Care must be taken to ensure that the summation of the DAQ acquisition duration (4 to 8 s) and the movement duration of translational stages (<2 s) do not exceed the duration between the two adjacent MTs. Hence, for this study, the MT was set to 0.1 to 0.05 Hz frequency (i.e., 10 to 20 s duration). The duration between the two MTs determined the duration between the two scanning locations and thereby the overall duration of the system scan.

2.3 *High-Intensity Focused Ultrasound Modulation*

The HIFU modulation is schematically displayed in the second row in Fig. 3. The shadowed areas represent that the HIFU is turned on and its duration is indicated as t_{on}. Otherwise, it means the HIFU is off. The period of each cycle (T) is also indicated and equal to the inverse of the modulation frequency ($1/f_{\text{M-HIFU}}$). The duty cycle is defined as the percentage of the HIFU is turned on in one cycle, which is t_{on}/T multiplied with 100%. The total HIFU exposure time (T_{on}) is equal to the product between t_{on} and the number of the cycles.

2.4 *Representations of Ultrasound-Switchable Fluorescence Signal Strength*

In our previous studies, a single HIFU exposure pulse (with a typical pulse width of 300 ms) was adopted.[11,12] The processing of previous USF data was as follows. The NI-DAQ card acquired the dynamic change of the amplitude of the 1-kHz signal before, during, and after the HIFU heating. The difference between the maximum amplitude and the background amplitude (acquired before HIFU exposure) was used as the USF signal strength at each location. After scanning the HIFU transducer or sample, an image was acquired based on the calculated USF strength.

In this study, because the HIFU exposure was different from that in our previous work,[11,12] the data acquisition and processing were different too. The time constant of the LIA-1 was kept at 10 ms when the HIFU modulation frequency ($f_{\text{M-HIFU}}$) was 1 and 2 Hz. The sensitivity of the LIA-1 was kept at 200 to 500 mV nA. The sensitivity of the Pre-Amp is set to 50 nA/V for low-noise mode.

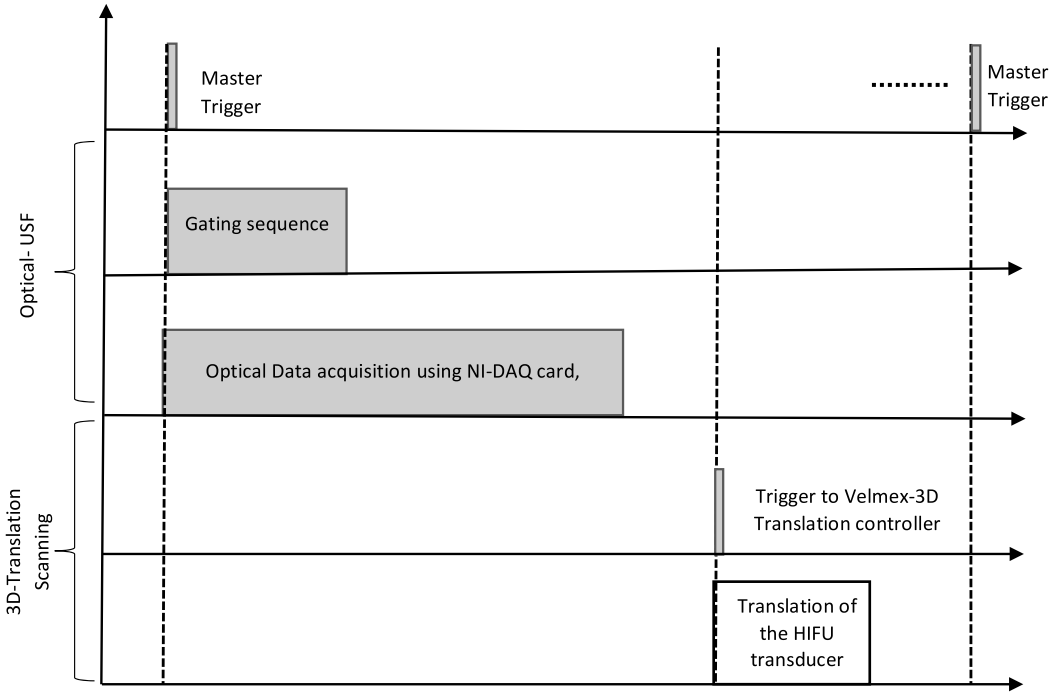

Fig. 2 A time sequence diagram of the operation of the USF imaging system.

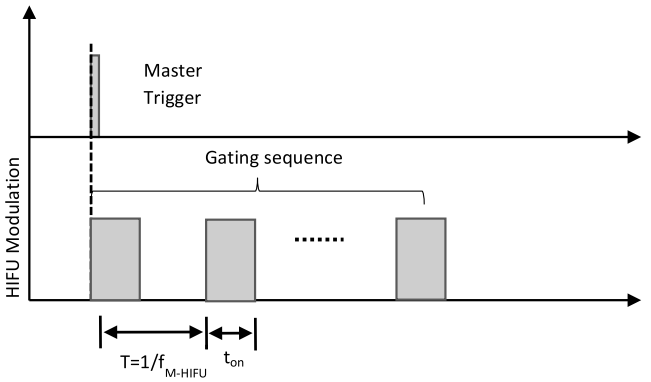

Fig. 3 A time sequence diagram to show the HIFU modulation and related parameters.

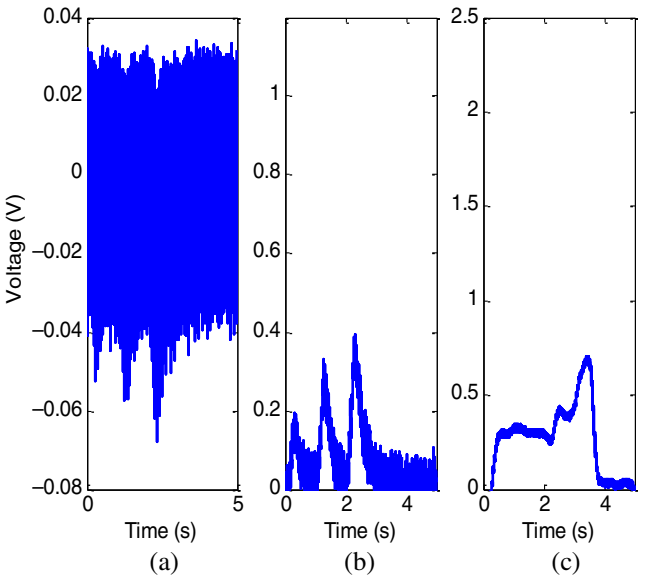

Fig. 4 An example to show the modulation of USF signal at 1 Hz with three cycles and a 10% duty cycle acquired from different locations: (a) acquired from the Pre-Amp, (b) acquired from the LIA-1, and (c) acquired from the LIA-2.

At each location of the HIFU transducer, three sets of data were simultaneously acquired. They were the data acquired from: (1) the Pre-Amp, which included the signals with both modulation frequencies ($f_{\text{M-OPT}}$ and $f_{\text{M-HIFU}}$); (2) the LIA-1, which was sensitive to the signal with the frequency of $f_{\text{M-OPT}}$ (i.e., 1 kHz) and detected its amplitude variation (at the frequency of $f_{\text{M-HIFU}}$); and (3) the LIA-2, which was sensitive to the signal with the frequency of $f_{\text{M-HIFU}}$ and detected its strength. The relationship among these three sets of data is shown in Fig. 4 and more details will be discussed in Sec. 3.

To quantify the USF strength at each location, Table 1 shows four methods (a to d) to process the acquired data. For data acquired from the Pre-Amp, the amplitude of the Fourier transform of the acquired signal at the frequency of $f_{\text{M-HIFU}}$ was adopted to represent the USF strength, which was the method (a) in Table 1 [Note that the raw signal acquired from the Pre-Amp is an amplitude-modulated (at the frequency of $f_{\text{M-HIFU}}$) sinusoidal wave (at a frequency of $f_{\text{M-OPT}}$)]. For data acquired from the LIA-1, the amplitude of its Fourier transform at the frequency of $f_{\text{M-HIFU}}$ was adopted to represent the USF strength, which was the method (b) in Table 1 (Note that the data acquired from the LIA-1 is a signal with a frequency of $f_{\text{M-HIFU}}$, which represents the amplitude profile of the signal from the Pre-Amp). For data acquired from the LIA-2, the maximum and the mean of the acquired signal (within a time window of the total duration of the HIFU exposure) were, respectively, used to represent the USF strength, which were the methods (c) and (d) in Table 1.

2.5 *Ultrasound-Switchable Fluorescence Contrast Agents*

The USF contrast agent used in this study was ADP(OH)_2-encapsulated Pluronic-F98 based thermos-sensitive nanocapsules. The details can be found in our previous publications.[12] The initial concentration of Pluronic-F98 in deionized water is 50 mg/ml. The peak excitation and emission wavelengths were around 680 and 715 nm, respectively. The temperature threshold (T_{th1}) is about 28°C, which is slightly lower than our previous results[11] and may be because of different fluorophores, some measurement errors and/or bench variation.

3 Results and Discussions

3.1 *Demonstration of Ultrasound-Switchable Fluorescence Modulation*

To demonstrate how the USF signal is modulated by the variation of HIFU exposure, we show a set of USF signals in Fig. 4, which were acquired, respectively, from the three different locations, as described above. Specifically, the HIFU was turned on and off at a frequency of 1 Hz ($f_{\text{M-HIFU}}$) with a duty cycle of 10% and a total duration of 3 s. This means within 1 s, the HIFU was turned on 0.1 s and off 0.9 s and this on-and-off cycle was repeated three times. To be able to clearly visualize

Table 1 Summary of the four methods to calculate USF signal strength. The letters (a)–(d) correspond to the figure sequence in Fig. 5.

Location where the signal was acquired	Method of processing the data for representing the USF strength	
Pre-Amp (a signal with a frequency of $f_{\text{M-OPT}}$ but the amplitude was modulated at a frequency of $f_{\text{M-HIFU}}$)	(a) The amplitude of the Fourier transform of the acquired signal at the frequency of $f_{\text{M-HIFU}}$	
LIA-1 (a signal with a frequency of $f_{\text{M-HIFU}}$, which represents the amplitude profile of the signal from the Pre-Amp)	(b) The amplitude of the Fourier transform of the acquired signal at the frequency of $f_{\text{M-HIFU}}$	
LIA-2 (a quasi direct current signal, which represents the amplitude profile of the signal from the LIA-1)	(c) The maximum of the acquired signal within the time window	(d) The mean of the acquired signal within the time window

the modulation of the USF signal, a relatively high SNR was adopted.

Figures 4(a), 4(b), and 4(c), respectively, show the acquired USF signals from the Pre-Amp, LIA-1, and LIA-2. The signal acquired from the Pre-Amp is an amplitude-modulated 1-kHz signal (i.e., $f_{\text{M-OPT}} = 1$ kHz and $f_{\text{M-HIFU}} = 1$ Hz). The amplitude modulation can be seen from the three large and negative peaks [Fig. 4(a)]. Note that the negative sign is caused by the PMT because usually a PMT generates a negative signal when optical intensity is increased. As discussed above, the LIA-1 functions as a demodulator to extract the variation of the amplitude of the 1-kHZ signal. Figure 4(b) clearly shows the 1-Hz USF signal with three cycles, which represents the profile of Fig. 4(a) after inverting the signal. Similarly, the LIA-2 functions as the second demodulator to extract the profile of the 1-Hz modulation signal. Figure 4(c) displays a quasi direct current signal, which represents the amplitude profile of the signal from the LIA-1 and proportional to the strength of the 1-Hz modulated USF signal.

3.2 *Ultrasound-Switchable Fluorescence Images*

Figure 5 shows the normalized 2-D USF images of a silicone tube (ID = 0.31 and OD = 0.64 mm) embedded in a piece of porcine muscle tissue with a thickness of ~12 mm. The 2-D USF images are obtained along the x–y plane across the silicone tube, as shown by the red dashed line in Fig. 1(c). Figures 5(a)–5(d), respectively, display the USF images processed using the four methods discussed in Tables 1 and 2. The details about the sample have been described in the section of the sample configuration. The HIFU modulation frequency is 2 Hz with a 10% duty cycle and a total of three cycles (controlled by FG-1). Thus, the total HIFU exposure time is 150 ms (i.e., the sum of three 50-ms on cycles). The driving signal of the HIFU is a 2.5-MHz sinusoidal waveform that is generated by FG-2, gated by FG-1, and amplified by RFPA. The peak-to-peak voltage of the driving signal from the FG-2 is ~0.1 V, and after being amplified 50 dB by the RFPA, the signal is ~32 V at the HIFU transducer.

Table 2 Calculated FWHMs and SNRs of USF images using different analysis methods.

	(a) FFT of USF signal	(b) FFT of LIA-1	(c) Max of LIA-2	(d) Mean of LIA-2	Non-modulation USF [11]
FWHM (mm)	0.95	0.95	1	0.96	~1.1
SNR	86	114	75	62	~40/ ~95

In general, all four methods clearly showed the tube via the modulation of USF. The full-width-at-half-maximum (FWHM) and SNR of each USF image were quantified and summarized in Table 2. The FWHMs of the USF images fall into the range from 0.95 to 1 mm, which is slightly larger than the tube OD and in agreement with our previous study.[11] This is because both studies used the same HIFU transducer, which is the major factor determining the USF resolution. The SNRs of these USF images in Fig. 5 are in the range from 62 to 114. The method (b) achieved the highest SNR of 114. Currently, it is unclear why the SNRs achieved by the methods of (c) and (d) are lower than the methods of (a) and (b). Further studies should be conducted to address this question in the future.

Unlike FWHM, these SNRs are higher than what we achieved in our previous study where no HIFU modulation was adopted and other experimental conditions were similar.[11] Specifically, in our previous study,[11] when the HIFU exposure was a single 300-ms burst (no modulation), the SNR was achieved ~40 in the similar sample using a time constant of 30 ms for LIA-1 (only one LIA was adopted in Ref. 11). After using a correlation method in our previous studies,[11] the SNR was improved from ~40 to ~95, which falls into the range of the current SNR values. This result indicates

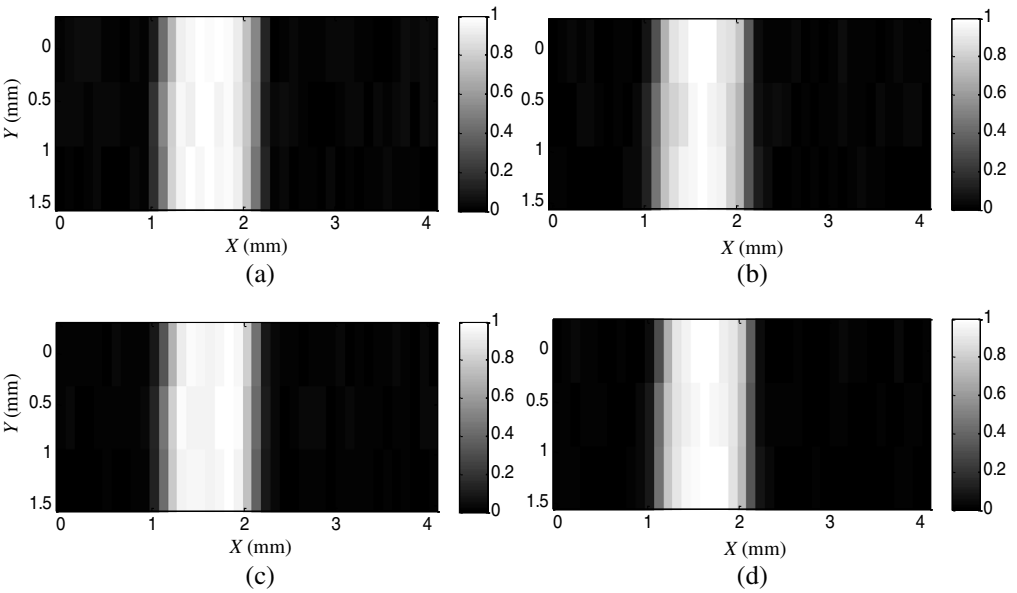

Fig. 5 Normalized 2-D USF images of the small tube embedded in the tissue sample. The images were processed using the four different methods of (a) to (d) in Tables 1 and 2. The HIFU modulation pattern is 2 Hz with a 10% duty cycle and a total of three cycles.

that the method developed in the current study (i.e., the modulation of USF) is comparable to the correlation method developed in our previous study.[11] Mathematically, this is understandable because both modulation and correlation follow the similar rule to recognize signals, which is to encode the USF signal with a unique temporal pattern and use a reference to extract the signal. The method of modulation encodes the USF signal with a specific frequency ($f_{\text{M-HIFU}}$) while the correlation method takes advantage of the natural dynamic change of the USF signal to differentiate the USF signal from the background noise. Note that the correlation method in our previous study[11] can be considered as a software-based off-line processing method, while the current method encodes the USF signal at a specific modulation frequency and can be considered a hardware-based online processing method. Another major difference is that the method of modulation has a specific modulation frequency so that the detection bandwidth may be narrower than that of the correlation method. Thus, the SNR (or sensitivity) of the modulation method should be relatively higher. If the SNR or sensitivity is similar, the applied HIFU power and/or exposure time should be lower or shorter. This is true if we compare the HIFU exposure parameters in our current and previous studies.[11] In the current study, the HIFU was turned on a total of 150 ms during a period of 1.5 s. In our previous study,[11] the HIFU was turned on a total of 300 ms while the HIFU exposure power is similar. Thus, the HIFU-induced temperature in the focal volume should be lower in the current study. Finally, we conclude that, compared with the nonmodulation method but processed with the correlation algorithm,[11] the current modulation method can achieve the similar SNR but shorten the HIFU exposure time by half. Furthermore, compared with the nonmodulation method without using the correlation algorithm, the current method not only achieves higher SNR but also uses shorter exposure time. Therefore, although the modulated HIFU exposure may lead to lower temperature rise compared with that of continuous wave HIFU exposure, the SNR may not be sacrificed because of the higher sensitivity.

3.3 *Effect of the Modulation Frequency ($f_{\text{M-HIFU}}$) and Duty Cycle on Ultrasound-Switchable Fluorescence Images*

Figure 6 shows the time sequence diagram of four different HIFU modulation patterns. Figures 6(a) and 6(b) have a modulation frequency of 1 Hz with a duty cycle of 10% and 20%, respectively. Figures 6(c) and 6(d) have a modulation frequency of 2 Hz with a duty cycle of 10% and 20%, respectively. There are three cycles for each HIFU exposure modulation. Figure 7 illustrates the normalized 2-D USF image acquired from the four HIFU exposure patterns. Note that these images were processed using the method of FFT of the LIA-1 output [method (b) in Table 1] since this method has relatively higher SNR in comparison to other methods.

The SNRs are summarized in Table 3 for the four different HIFU modulation exposures. For $f_{\text{M-HIFU}} = 1$ Hz, when increasing the duty cycle from 10% to 20% [i.e., from (a) to (b) in Table 3], all the SNRs acquired from the four processing methods increase obviously and consistently. This result can be explained using the concept of temperature modulation depth, which is usually defined as the ratio between the difference and the sum of the maximum and minimum temperature values. The above result indicates that the modulation depth of the HIFU-induced temperature increases with the increase of the duty cycle for these two cases. This is understandable because the higher duty cycle means longer HIFU exposure time for each cycle and therefore higher temperature rise and stronger USF signals. On the other hand, the time period when HIFU remains off is longer enough for these two cases to allow the temperature decreasing to generate the modulation pattern. This is because the modulation frequency is 1 Hz and the time period when HIFU remains off in each cycle is 0.9 and 0.8 s for the 10%

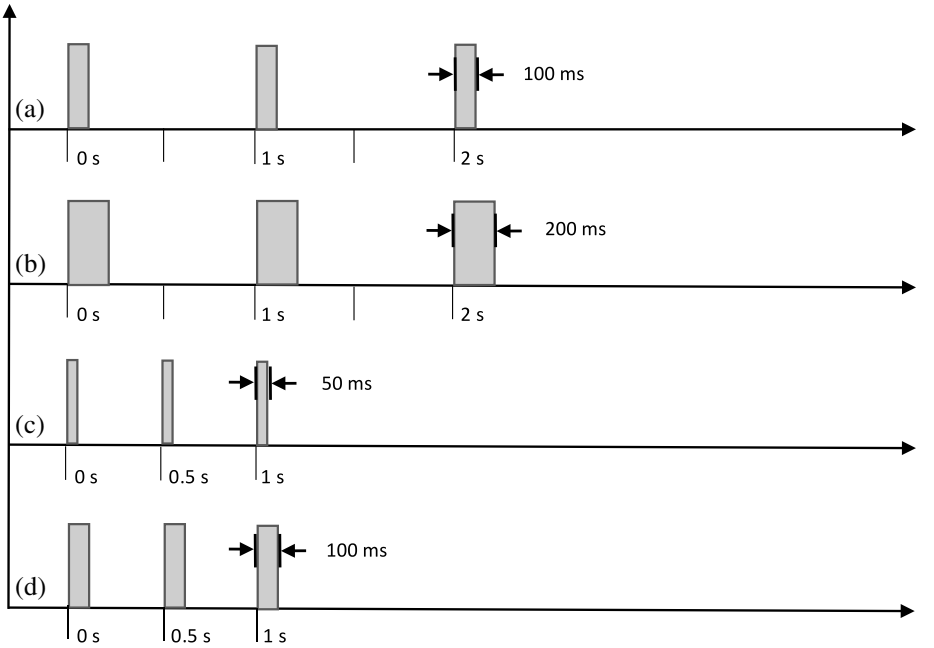

Fig. 6 The time sequence diagram of four different HIFU modulation patterns: (a) 1 Hz with a 10% duty cycle, (b) 1 Hz with a 20% duty cycle, (c) 2 Hz with a 10% duty cycle, and (d) 2 Hz with a 20% duty cycle. All modulation patterns have three cycles.

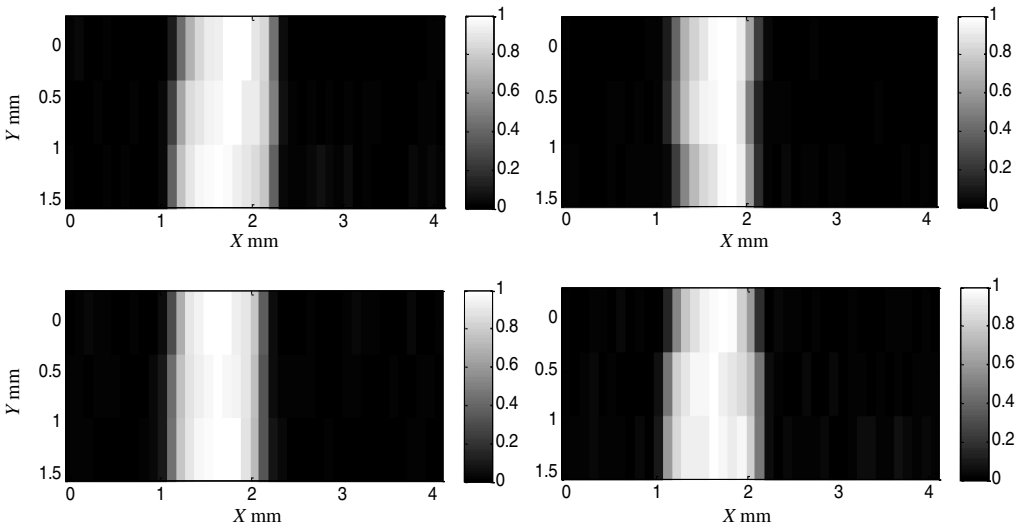

Fig. 7 Normalized 2-D USF images of the small tube embedded in the tissue sample with four different HIFU modulation patterns: (a) 1 Hz with a 10% duty cycle, (b) 1 Hz with a 20% duty cycle, (c) 2 Hz with a 10% duty cycle, and (d) 2 Hz with a 20% duty cycle. All modulation patterns have three cycles. The images were processed by using the method of the FFT of the LIA-1 signal.

Table 3 Calculated SNRs of USF images using the different analysis methods at different HIFU modulation exposures.

	(a) FFT of USF signal	(b) FFT of LIA-1	(c) Max of LIA-2	(d) Mean of LIA-2
(a) 1 Hz-10%-three cycles	76	144	67	50
(b) 1 Hz-20%-three cycles	152	175	87	65
(c) 2 Hz-10%-three cycles	86	114	75	62
(d) 2 Hz-20%-three cycles	77	90	61	43

and 20% duty cycle, respectively. Both values are usually longer than the thermal diffusion time constant in the adopted tissue phantom. Thus, the difference between the maximum and minimum temperature is large, which leads to large modulation depth and therefore high SNR.

However, when the HIFU modulation frequency increases to 2 Hz, raising the duty cycle from 10% to 20% [i.e., from (c) to (d) in Table 3] leads to slight and consistent decrease of SNRs. This result indicates that the modulation depth is reduced when increasing the duty cycle for 2-Hz exposure. This may be because the time period when HIFU remains off is not long enough to allow the temperature decreasing. For the modulation frequency of 2 Hz, the time period when the HIFU remains off in each cycle is 0.45 and 0.4 s for the 10% and 20% duty cycle, respectively. These two values may be close to the thermal diffusion time constant in the adopted tissue phantom. Thus, reducing the time period of off-cycle will limit the cooling time and therefore, the temperature may not be able to reduce down enough. Accordingly, both the modulation depth and SNR reduce.

Comparing all four modulation patterns, the SNRs achieve the highest level for all four processing methods when $f_{\text{M-HIFU}} = 1$ Hz with the 20% duty cycle [i.e., (b) in Table 3]. By contrast, the SNRs fall down to the lowest level when $f_{\text{M-HIFU}} = 2$ Hz with the 20% duty cycle [i.e., (d) in Table 3]. Last, the SNRs of the remaining two cases [i.e., (a) and (c) in Table 3] are in between and also their SNRs are comparable. Therefore, the modulation pattern (a), $f_{\text{M-HIFU}} = 1$ Hz with the 20% duty cycle, is the best choice for this study. In addition, comparing all four processing methods, the FFT of the signal from the LIA-1 always provides the highest SNRs, followed by the methods of the FFT of the filtered USF signal. The SNRs of the remaining two methods, where two LIAs were used, are relatively lower for all the four HIFU exposure patterns. The reasons are unclear and should be investigated in the future.

4 Conclusion

An innovative USF imaging method is developed in this study by modulating HIFU exposure at a specific frequency ($f_{\text{M-HIFU}} = 1$ to 2 Hz) with a small duty cycle (10% to 20%). Thus, the temperature at the HIFU focal volume is modulated, which leads to the modulation of USF signal at the same modulation frequency. By specifically detecting this USF signal, the SNR of the USF image (or equivalently the detection sensitivity) should be significantly improved. The modulation of the USF signal has been clearly demonstrated. Compared with our previous methods (without modulation and without processing by the correlation method), the SNR is significantly improved. A total of four HIFU modulation methods and four signal processing methods have been investigated. The highest SNR level is achieved by modulating the HIFU at $f_{\text{M-HIFU}} = 1$ Hz with the 20% duty cycle and processed by using FFT of the signal from the LIA-1.

Disclosures

The authors have no relevant financial interests in this article and no potential conflicts of interest to disclose.

Acknowledgments

This work was supported in part by funding from the NSF CBET-1253199 (B.Y.), the CPRIT RP170564 (B.Y.) and 120052 (B.Y.), and the NHARP 13310 (B.Y.).

References

1. D. M. McDonald and P. L. Choyke, "Imaging of angiogenesis: from microscope to clinic," *Nat. Med.* **9**, 713–725 (2003).
2. L. V. Wang, "Multiscale photoacoustic microscopy and computed tomography," *Nat. Photonics* **3**, 503–509 (2009).
3. L. H. V. Wang and S. Hu, "Photoacoustic tomography: in vivo imaging from organelles to organs," *Science* **335**, 1458–1462 (2012).
4. L. H. V. Wang, "Ultrasound-mediated biophotonic imaging: a review of acousto-optical tomography and photo-acoustic tomography," *Dis. Markers* **19**, 123–138 (2003).
5. Y. Lin et al., "Temperature-modulated fluorescence tomography based on both concentration and lifetime contrast," *J. Biomed. Opt.* **17**, 056007 (2012).
6. Y. Lin et al., "Temperature-modulated fluorescence tomography in a turbid media," *Appl. Phys. Lett.* **100**, 73702–737024 (2012).
7. B. Yuan et al., "High-resolution imaging in a deep turbid medium based on an ultrasound-switchable fluorescence technique," *Appl. Phys. Lett.* **101**, 033703 (2012).
8. S. Yu et al., "New generation ICG-based contrast agents for ultrasound-switchable fluorescence imaging," *Sci. Rep.* **6**, 35942 (2016).
9. Y. B. Pei et al., "High resolution imaging beyond the acoustic diffraction limit in deep tissue via ultrasound-switchable NIR fluorescence," *Sci. Rep.* **4**, 4690 (2014).
10. B. B. Cheng et al., "Development of ultrasound-switchable fluorescence imaging contrast agents based on thermosensitive polymers and nanoparticles," *IEEE J. Sel. Top. Quantum Electron.* **20**, 6801214 (2014).
11. B. B. Cheng et al., "High-resolution ultrasound-switchable fluorescence imaging in centimeter-deep tissue phantoms with high signal-to-noise ratio and high sensitivity via novel contrast agents," *PLoS One* **11**, e0165963 (2016).
12. J. Kandukuri et al., "A dual-modality system for both multi-color ultrasound-switchable fluorescence and ultrasound imaging," *Int. J. Mol. Sci.* **18**, 323 (2017).
13. B. Cheng et al., "The mechanisms and biomedical applications of an NIR BODIPY-based switchable fluorescent probe," *Int. J. Mol. Sci.* **18**, 384 (2017).
14. A. Corlu et al., "Three-dimensional in vivo fluorescence diffuse optical tomography of breast cancer in humans," *Opt. Express* **15**, 6696–6716 (2007).

Jayanth Kandukuri received his BTech degree in biomedical engineering from JNTU, Telangana, India, in 2005, his ME degree in electronic engineering from UQ, Australia, in 2007, and his MSc degree in bioengineering from UT at Arlington, United States, in 2012. He worked as a Jr. biomedical engineer in CARE Hospital Ltd., India, from 2008 to 2010. His research interests include tissue ultrasound and optical imaging.

Shuai Yu received his bachelor of science degree in biotechnology from Zhejiang Sci-Tech University, Zhejiang, China, in 2012, and master of engineering degree in biomedical engineering from the University of Southern California, United States, in 2014. His research interests include tissue ultrasound and optical imaging.

Tingfeng Yao received his BS degree in electronic information science and technology from Nanjing University of Aeronautics and Astronautics, Nanjing, China, in 2012, and his MS degree in electromagnetic field and microwave technology from Nanjing University of Aeronautics and Astronautics, Nanjing, China, in 2015. He is currently working toward his PhD degree in bioengineering at the University of Texas at Arlington, United States. His current research interest is developing ultrasound-switchable fluorescence imaging technique.

Baohong Yuan received his PhD degree in biomedical engineering from the University of Connecticut, Storrs, Connecticut, United States, in 2006. He is currently an associate professor of biomedical engineering at the University of Texas at Arlington, Arlington, Texas, United States. His research interest is to explore and develop new imaging technology, including contrast agents and instruments, for understanding cancer mechanisms, early detecting and diagnosing cancers, and monitoring cancer treatment efficiency.